NUMERICAL STUDY OF SWIRLING FLOW IN A LIQUID-LIQUID AXIAL HYDROCYCLONE SEPARATOR

André D. Rocha, damiani@dep.fem.unicamp.br
Antonio C. Bannwart, bannwart@dep.fem.unicamp.br
State University of Campinas – UNICAMP-FEM-DEP
Dept. of Petroleum Engeneering
Cidade Universitária – B. Geraldo
13083-970 – Campinas-SP-Brazil

Macelo M. Ganzarolli, ganza@fem.unicamp.br
State University of Campinas – UNICAMP-FEM-DE
Dept. of Energy
Cidade Universitária – B. Geraldo
13083-970 – Campinas – SP - Brazil

Erick F. Quintella, erickquintella@petrobras.com.br
Petrobras – E&P
Av. Chile, 65 – sala 912
20031-912 – Rio de Janeiro - RJ

Abstract. *Cyclone separators use swirling flow to provide a sorting mechanism to segregate dispersed material from within a carrier fluid. Large centrifugal forcres can be created by the swirling motion depending upon the density difference, cyclone diameter and flow rate. Compact oil-water-gas separators are often required in process industry and are essential in offshore petroleum production. In this work oil-water hydrocyclones are studied. A compact design is provided by the axial hydrociclone, which takes advantage of the pipe geometry of the incoming oil-water mixture. A flow pattern of small water droplets dispersed into a continuous oil phase can be assumed for the incoming flow. The swirl motion is generated by a system of fixed axial vanes. If the oil is relatively viscous, the incoming flow can be assumed to be laminar for moderate flow rates. By means of CFD, velocity profiles and pressure distributions past the swirl generator are determined for several geometries and flow conditions. The numerical study is aimed at determining the length for which swirl motion decays as a function of the flow and geometry variables involved. The decay length is compared with an approximate expression for the length required to segregate water droplets, as a criterium to assess the viability of a particular design.*

Keywords*: Swirling Flow; Hydrocyclone; Liquid-Liquid Separator; Computational Fluid Dynamics*

1. INTRODUCTION

Cyclones are used in various industries to separate two components of different densities with the help of centrifugal forces created by the swirling flow. It is common to find solid-liquid and solid-gas cyclones in industry, but in the case of two immiscible liquids the application of hydrocyclones is less common due to the small density difference between the phases. One exception to this is the oil industry in which hydrocyclones are used to remove oil from the produced water before the aqueous phase is disposed overboard or re-injected into the formation.

The design of cyclones in general is still largely based on geometrical relationships and correlations derived from time consuming experimental studies in a specific geometry or geometries (Young *et al*., 1994). In a conventional cyclone the mixture to be separated enters the separation chamber via one, or sometimes more tangential inlets. Although the axial cyclone is less common, a number of designs can be found in several industrial applications, e.g. liquid removal from gas streams (Swanborn, 1988), solid/dust removal from gas (Klujszo *et al*., 1999). But the application of axial hydrocyclones to liquid-liquid separation is very rare (Dirkzwager, 1996; Delfos and Dirkzwager, 1998). In principle, it consists of a pipe geometry as illustrated in Fig. 1. The flow along the axial hydrocyclone is put into rotation by a swirl generator device. This is a cylindrical body centered in the pipe, on which vanes are mounted in order to provide a tangential velocity component to the incoming axial flow. The difficulty in designing efficient hydrocyclones lies in the broad range of industrial applications, where for each set of physical operational parameters there is supposedly a different optimal geometry.

With the help of numerical simulations, many studies have been performed to investigate the flow in axial separators for strongly swirling turbulent flow. Keege (2000) performed a numerical analysis of turbulent flow to improve the axial hydrocyclone separator geometry investigated by Dirkzwager (1996). The study focused on explaining the difference between the simulations and experimental results and discussed the usefulness of the commercial package

utilized (CFX) for cyclone designing purposes. He concluded that the Differential Reynolds Stress Model (DRSM) is the best method for simulating turbulent swirling flows using the Reynolds averaged Navier-Stokes (RANS) approach. Delfos (2004) developed a numerical model for liquid-liquid turbulent flow (called HAAS) to predict the velocity field in axi-symmetric flows with high swirl and Reynolds numbers in cyclone geometries. The results were compared with both simulations using a commercial CFD code (Fluent) and results from laboratory experiments. It was concluded that the HAAS model is very time-efficient in the design of axial hydrocyclones and can be used as an interactive tool with real-time output.

A comparative study between two commercial CFD-packages (CFX 4.3 and Fluent V6.0.12) for a straight tube hydrocyclone in strongly swirling single-phase flow (Murphy *et al*., 2004) showed that both models give qualitatively good results, although they differ significantly in the core region. Both CFD codes were found to be very sensitive to the choice of turbulence modeling parameters.

No investigation on viscous effects in axial hydrocyclones was found, although viscosity may play an important effect for heavy oils containing small dispersed water droplets. In this paper we numerically investigate the laminar swirling flow in the downstream portion of the swirl generator, i.e. the so-called separation section or settling zone shown in Fig. 1. The numerical study is aimed at determining the length for which swirl motion decays as a function of the flow and geometry variables involved. The decay length is compared with an approximate expression for the length required to segregate water droplets, as a criterium to assess the viability of a particular design.

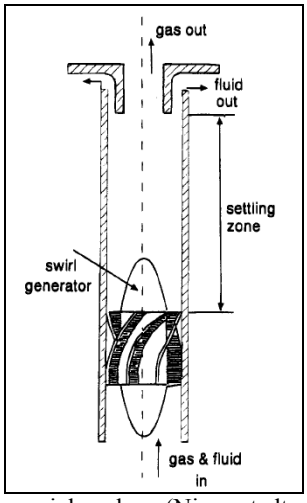

Figure 1. Schematics of an axial cyclone (Nieuwstadt and Dirkzwager, 1995)

2. FLOW GEOMETRY

Two geometries were studied. CASE#1 has only a central cone of length L_c and radius r_c at the inlet of the settling zone, whereas CASE#2 has a central cone followed by a cylindrical core of lengh L_{SC} and radius R_{SC}. Those geometries are illustrated in Figure 2.

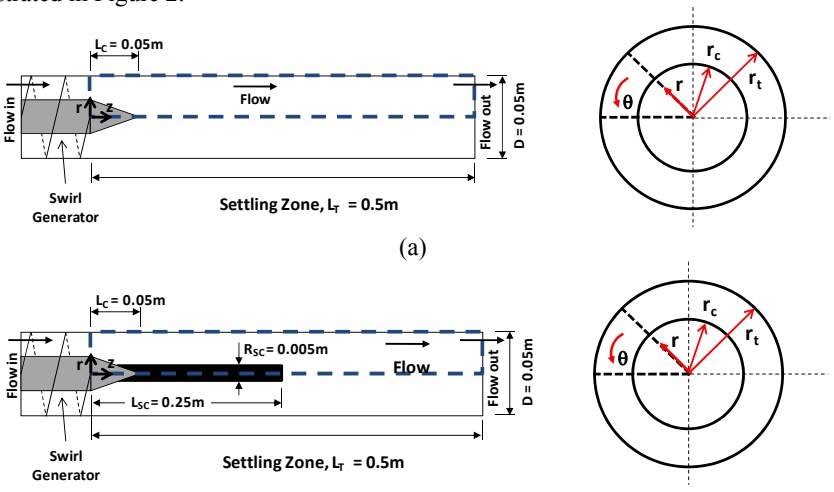

Figure 2. Investigated geometries: (a) Case#1 and (b) Case#2.

3. COMPUTATIONAL MODEL

The behavior of the flow is in general governed by the fundamental principles of classical fluid mechanics expressing the conservation of mass and momentum.

3.1. Governing Equations

The continuity and momentum dimensionless equations for steady state, incompressible, isothermal and axisymmetric flow in cylindrical coordinates (r, θ, z) with $V_r = v$; $V_\theta = u$; $V_z = w$, are given below:

Continuity:

$$\frac{1}{r^*}\frac{\partial}{\partial r^*}(r^* v^*) + \frac{\partial w^*}{\partial z^*} = 0 \tag{1}$$

Axial Momentum:

$$v^*\frac{\partial w^*}{\partial r^*} + w^*\frac{\partial w^*}{\partial z^*} = -\frac{\partial p^*}{\partial z^*} + \frac{2}{\mathrm{Re}}\left[\frac{1}{r^*}\frac{\partial}{\partial r^*}\left(r^*\frac{\partial w^*}{\partial r^*}\right) + \frac{\partial^2 w^*}{\partial z^{*2}}\right] \tag{2}$$

Radial Momentum:

$$v^*\frac{\partial v^*}{\partial r^*} + w^*\frac{\partial v^*}{\partial z^*} - \frac{u^{*2}}{r^*} = -\frac{\partial p^*}{\partial r^*} + \frac{2}{\mathrm{Re}}\left[\frac{1}{r^*}\frac{\partial}{\partial r^*}\left(r^*\frac{\partial v^*}{\partial r^*}\right) + \frac{\partial^2 v^*}{\partial z^{*2}} - \frac{v^*}{r^{*2}}\right] \tag{3}$$

Tangential Momentum:

$$v^*\frac{\partial u^*}{\partial r^*} + w^*\frac{\partial u^*}{\partial z^*} + \frac{v^* u^*}{r^*} = \frac{2}{Re}\left[\frac{1}{r^*}\frac{\partial}{\partial r^*}\left(r^*\frac{\partial u^*}{\partial r}\right) + \frac{\partial^2 u^*}{\partial z^{*2}} - \frac{u^*}{r^{*2}}\right] \tag{4}$$

where Re = $\rho W_{avg} D/\mu$, W_{avg} is the average axial velocity over the cyclone cross section of diameter D and $p^* = p/\rho W_{avg}^2$

3.2. Boundary Conditions

Accounting for the results obtained by Nieuwstadt and Dirkzwager (1995) for the optimum geometry of the vanes, we assumed that at the inlet of the separator section ($z = 0$) the tangential velocity component (u) is twice the axial component (w), ie, $\alpha = 63{,}43^o$. At r = R = D/2 the non-slip condition is used in the wall and at r = 0, $\partial/\partial r = 0$. The average axial component (W_{avg}) was transformed into a Reynolds number (Re) by rewriting the momentum equations in dimensionless form. Besides, every velocity component vanishes at the walls. The annular thickness ratio, $\delta^* = (r_t - r_c)/r_t$, was set to 0.16; 0.28 and 0.4. Fluid properties were set 300 mPa.s and 937.8 kg/m^3. All simulations were performed for laminar flow ($Re \leq 2000$). Table 1 shows the boundary conditions adopted.

Table 1: Boundary Conditions

Inlet	Outlet	At r = 0	Wall (at r = R)
$U_{in} = W_{in}/tg(\alpha)$	$\frac{\partial u}{\partial z} = 0$	$\frac{\partial u}{\partial r} = 0$	$u = 0$
$V = 0$	$\frac{\partial v}{\partial z} = 0$	$\frac{\partial v}{\partial r} = 0$	$v = 0$
$W_{in} = \frac{\mathrm{Re}\,\mu}{\rho D}\left[\frac{A}{A_{in}}\right]$	P_{rel}	$\frac{\partial w}{\partial r} = 0$	$w = 0$

The governing equations were discretized and solved using the finite volume method (Patankar, 1980) by means of the CFD package Phoenics®. The pressure correction was achieved with SIMPLEST, which is a derivative of SIMPLE. For diffusive and convective terms were discretized using hybrid scheme. The mesh was choosed after to test three meshes. The better results *versus* computational-time was obtained for mesh 5x20x120. This mesh is used in all simulations in this paper.

4. RESULTS AND DISCUSSION

4.1. Tangential Velocity

The flowfield of swirling flow is governed by the behavior of the tangential component. The magnitude of the near-wall tangential velocity decreased with distance which can be explained by swirl decay and viscous fluid flow. Figure 3 illustrates the profile of the tangential velocity component for Case#1 geometry with different annular ratios at two axial positions: z = 1D (Fig. 3-a) and z = 5D (Fig. 3-b). It can be observed that the swirl component increases with the radial position in the central region (as in a forced vortex), attains a maximum then decreases as the wall is approached. This behavior is not interesting for separating particles concentrated in the central region of the cyclone. On the other hand, thinner annular gaps tend to generate higher tangential velocity peaks, but somewhat lower values in the central region. This agrees with the findings of Nieuwstadt and Dirkzwager (1995) according to which the annular thickness is greatly important for the separation efficiency of the axial hydrocyclone, as will be discussed later in sub-section 4.3. On the other hand, the swirl decays significantly with the axial position, which is also due to the viscosity.

4.2. Axial Velocity

The development of the axial velocity downstream is shown in Fig. 4 for the same conditions of Fig. 3. At z = 1D (Fig. 4-a) low axial velocities occur near the center due to the conic core. At z = 5D a central recirculation zone exists due to strong radial and axial pressure gradients caused by the expanding flow cross section area.

An illustration of the recirculation zone is shown in Fig. 5. The magnitude of the backflow is observed to increase from 2.8D until to the end of the tubing. Although Murphy *et al*. (2007) has studied the turbulent swirling flow they also observed the formation of a central recirculation zone.

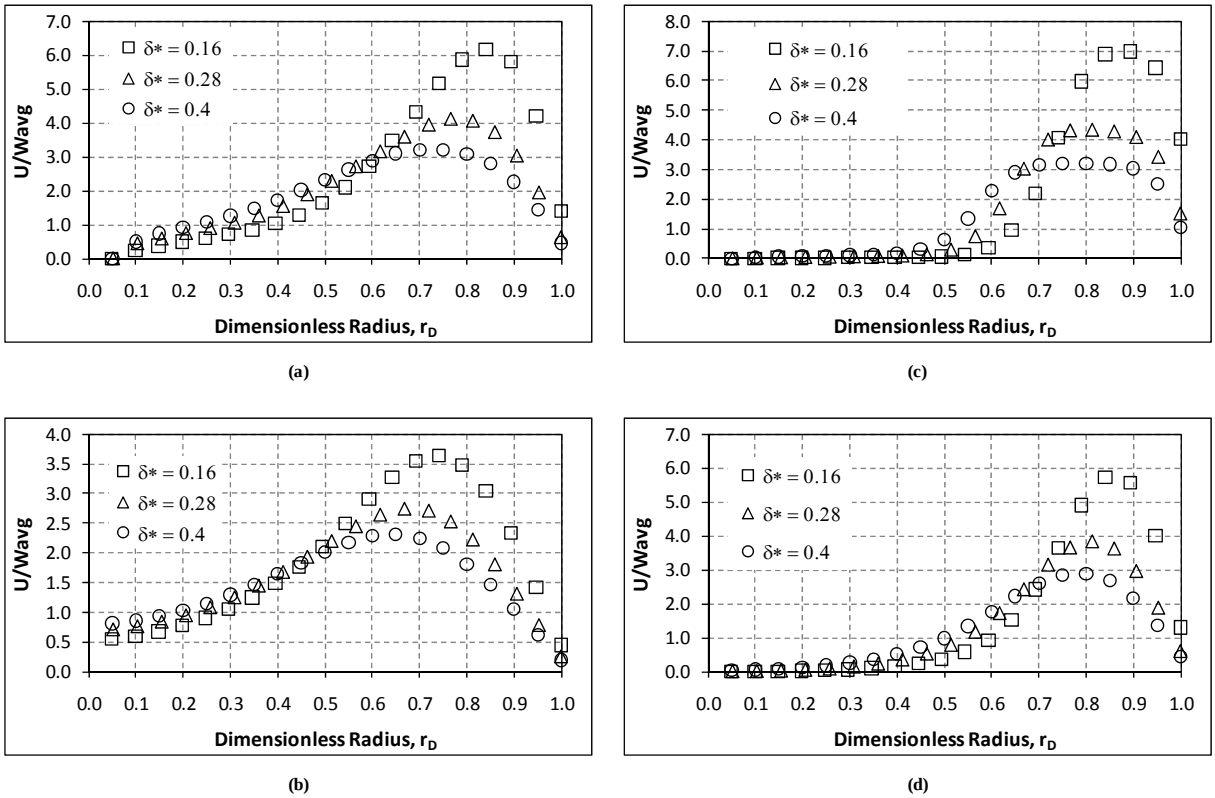

Figure 3: Tangential velocity profile: Re = 500, (a) z = 1D, (b) z = 5D; Re = 2000, (c) z = 1D, (d) z = 5D.

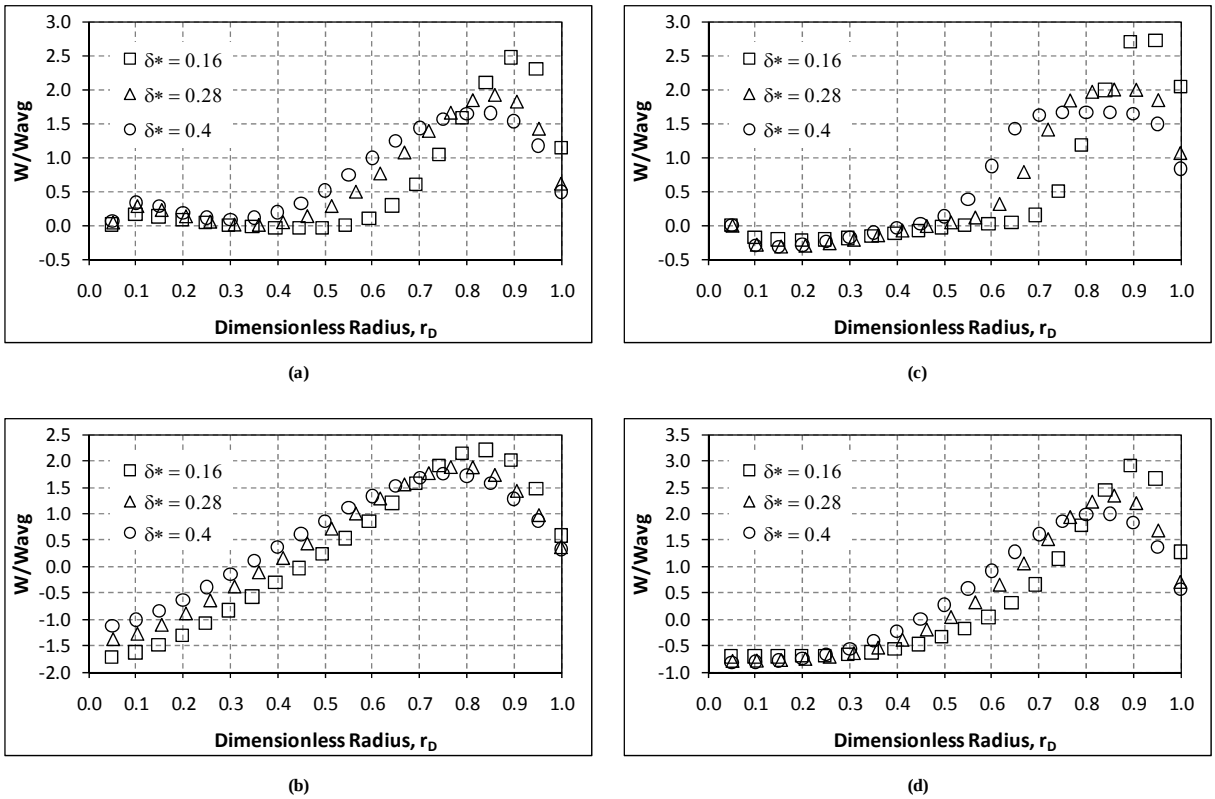

Figure 4. Axial velocity profile: Re = 500, (a) z = 1D, (b) z = 5D; Re = 2000, (c) z = 1D, (d) z = 5D.

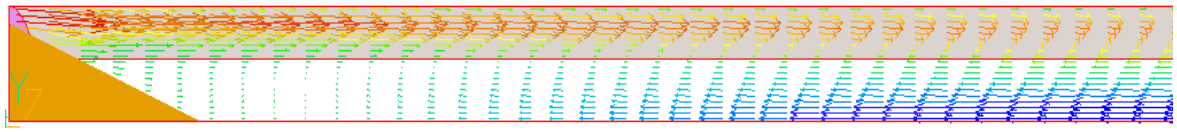

Figure 5. Recirculation zone for Case#1 geometry at Re = 500 and δ* = 0.16.

4.3. Separation Length

From a balance between Stokes drag and centrifugal force but assuming a potential flow velocity distribution for the tangential component, Nieuwstadt and Dirkzwager (1995) derived the following result for the separation length:

$$\frac{L_S}{D} = \frac{5.652(\delta / a)^2}{\mathrm{Re}} \tag{5}$$

For a particle of diameter 100 μm and Re = 500 this results in a separation length of nearly 6 m for δ = 1 cm and D = 5 cm, i.e., L_S/D = 113. However, the assumption of potential velocity distribution is not consistent with Fig. 3 once the flow here is laminar and tangential velocity distribution approaches the one of a forced vortex.

4.4. Swirl Number

For engineering purposes it is important to understand the decay process of swirl intensity along the pipe. Since the swirling flow tends to have large-scale effects on flow field, Gupta *et al*. (1984) recommends the use of the dimensionless swirl number, S, to characterize the flow. In this work the definition adopted by Kitoh (1991) and Dirkzwager (1996) was used:

$$S = \frac{2\int_0^R wur^2 dr}{R^3 W_{avg}^2} \tag{6}$$

The swirl number is a dimensionless number that expresses the ratio of the axial flux of tangential momentum to the axial flux of axial momentum, thus it gives a measure of the strength of the swirling flow. As the flow develops downstream, wall friction reduces both the axial and tangential momentum fluxes in the near wall region (Baker and Sayre, 1971; Kitoh, 1991; Senoo and Nagata, 1972; Sheen *et al*., 1996), thus causing swirl decay. Figure 6 shows the swirl decay as a function of axial distance. As observed in Fig. 3, the smaller the annular thickness the higher the peak in the tangential velocity. At z ≅ 8D the swirl number is still 0.25 for $\delta^* = 0.16$ but vanishes for $\delta^* = 0.4$. In the present study, viscosity plays a prominent effect in swirl decay.

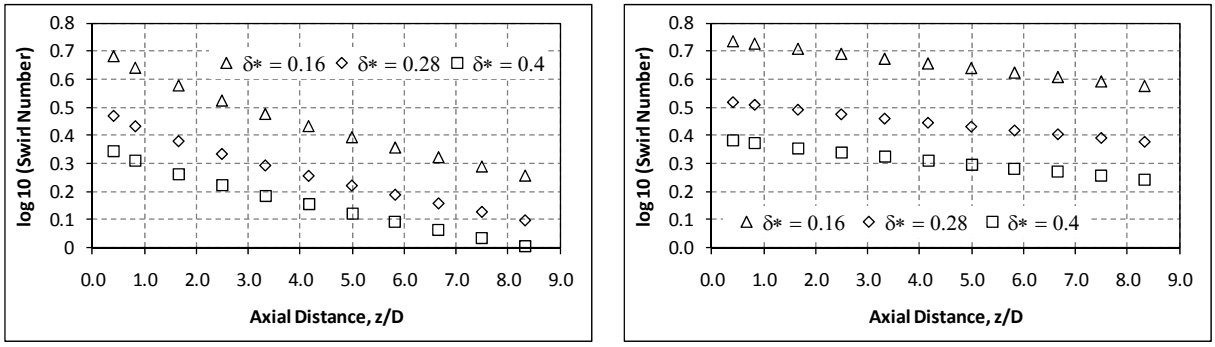

Figure 6. Swirl number decay with axial position at several annular thickness ratios, (a) Re = 500 and (b) Re = 2000.

4.5. Pressure Distribution (inserir a definição de P após a equação 4)*

It is well-know that in a swirling pipe flow the radial distribution of pressure is different in the downstream direction with the decay of swirl. Such pressure profiles give important information not only about the decay of swirl but also the energy loss in swirling flow. The dimensionless pressure distributions shown in Fig. 7 again indicate the advantage of using a small annular thickness ratio, since this design provides the lowest pressure drop.

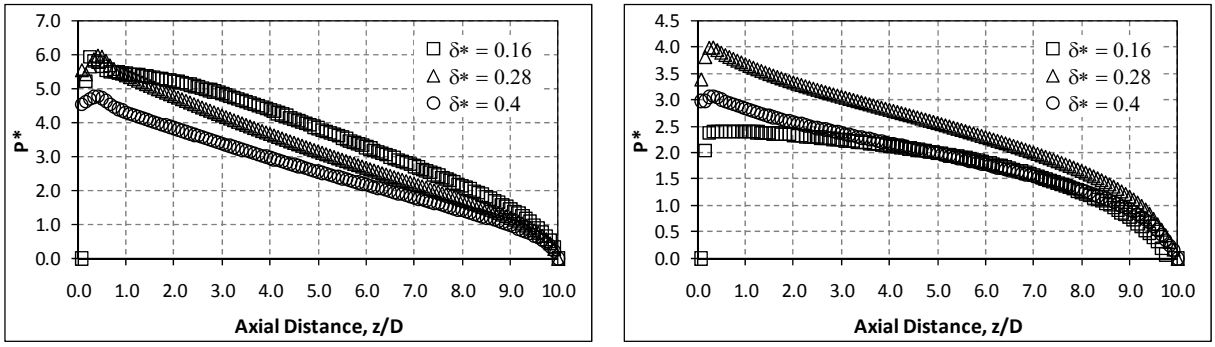

Figure 7. Pressure distribution, (a) Re = 500 and (b) Re = 2000.

4.6. Comparison Between Geometry Cases #1 and #2

The addition of a cylindrical section following the conical core was initially intended to reduce the dissipation near the pipe axis. Figure 8 presents results of comparison between Cases #1 and #2. The centerline pressure is shown in Fig. 8-a for both geometries. It can be seen that Case #2 seems to provide a more constant pressure along the hydrociclone, thus it seems preferable. Besides, it significantly reduced the recirculation observed in Case#1. However the profiles of tangential and axial velocity components in Figs. 8-b and 8-c are not very different. Results for the swirl decay shown in Fig. 8-d are nearly the same for both geometries.

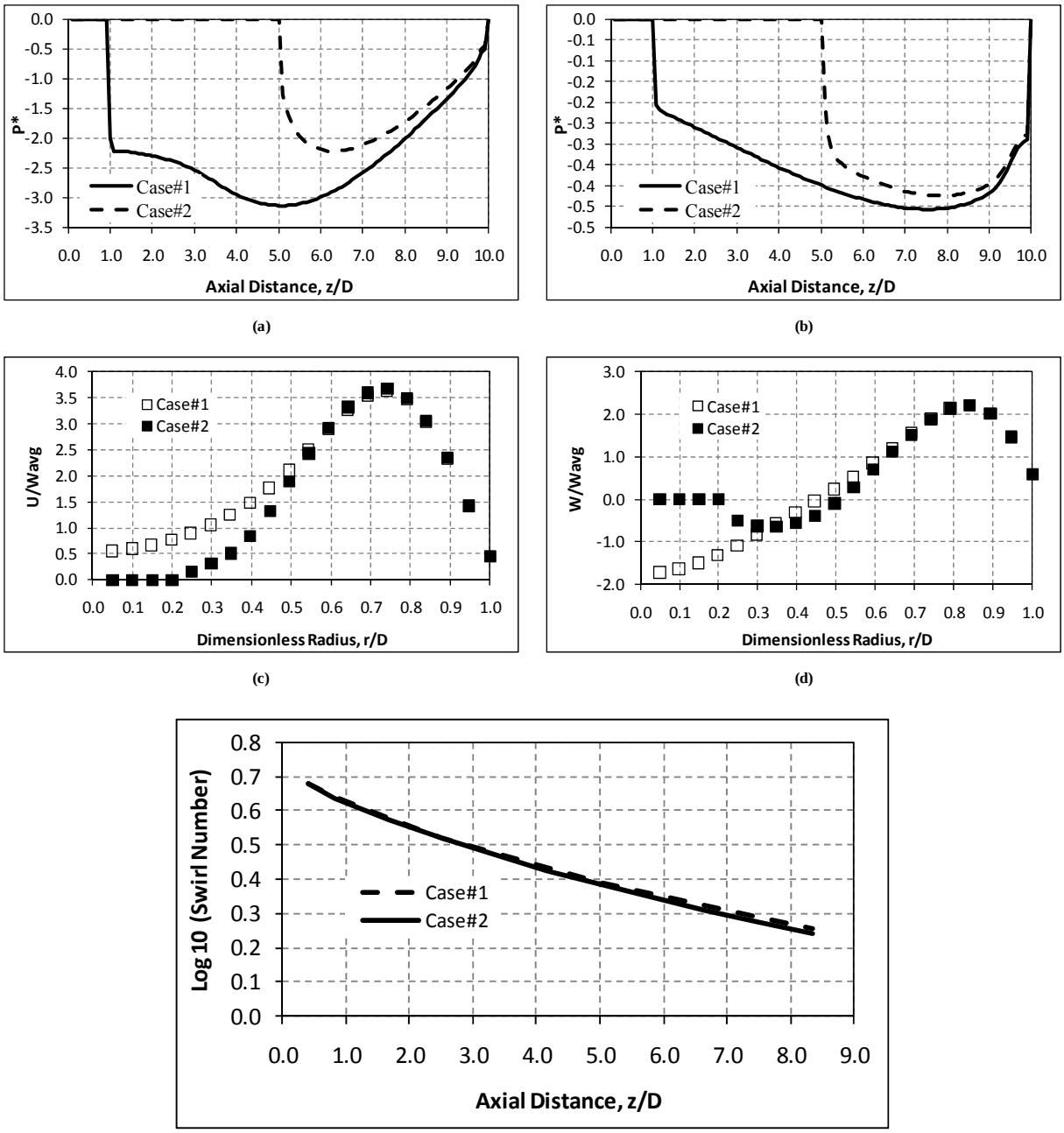

Figure 8. Comparative results between Cases #1 and #2 at Z = 5D: Centerline pressure drop for δ* = 0,16 (a) Re = 500 and (b) Re = 2000. For Re = 500, (c) tangential velocity,(d) axial velocity and, (e) Swirl number.

Due to the vortex stretching the axial vortivity along the center line increases, shown in Fig 5. The magnitude of the backflowing axial velocity increased from 2.8D until to the end of the tubing. Murphy (2007) studied the turbulent swirling flow and noted that recirculation too. This phenomenon occurs because the fluid slows down in the center creating an adverse pressure gradient. However, a break-up process due to recirculation will produce smaller droplets and these can no longer be handled by a cyclone. Dirkzwager (1996) designed a geometry to avoid this recirculation that showed other benefits too. Thus we decided to run further simulations for a geometry similar to Dirkzwager's, which is shown in Figure 9.

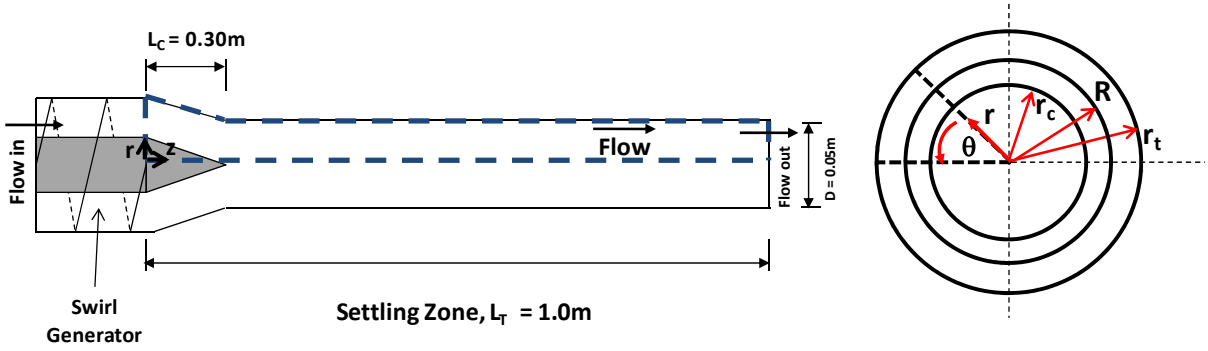

Figure 9: Dirkzwager geometry, with r_c = 0.055m, r_t = 0.065m and r_{ti} = 0.025m.

Using this geometry, except for inlet cone, after running simulations in laminar flow (Re ≤ 2000) we noted that the recirculation disappeared. Figure 10 shows comparative results between Dirkzwager's geometry and Cases #1 and #2.

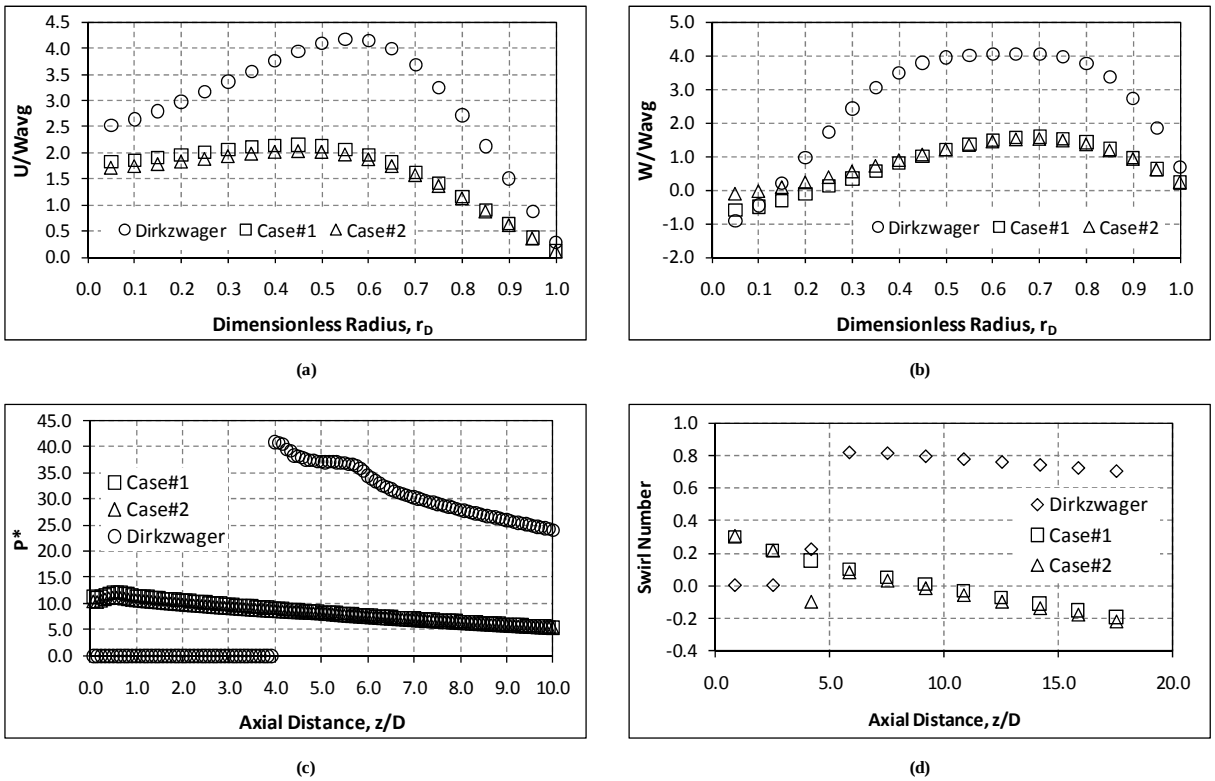

Figure 10: Comparative results between Dirkzwager and Cases #1 and #2 for δ* = 0,4 and Re = 500. (a) Tangential velocity and, (b) Axial velocity at Z=10D; (c) Pressure drop and (d) Swirl number.

Figure 11 shows the axial velocity vectors for Dirkzwager's geometry. Note that recirculation is much lower and axial velocity much higher than Case#1.. Furthermore, the tangential velocity is much higher than the previous geometries, indicating a better separation performance.

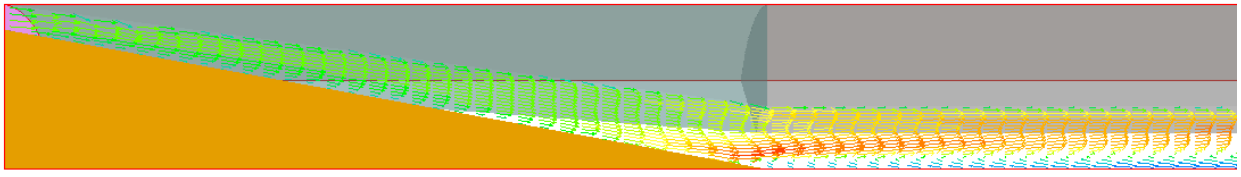

Figure 11: Axial velocity vector for Dirkzwager geometry.

5. CONCLUSIONS

In the present work different geometries for an axial hydrocyclone intended for liquid-liquid separation were numerically studied by means of CFD. The flow was assumed to be laminar for applications in heavy oil-water separation. The simulations indicated that, besides viscosity, the annular thickness has a strong influence on the velocity profiles, pressure and swirl number. The comparison between the geometries indicated that Case#2 presents some advantage in keeping pressure nearly constant in the separator but in both cases the recirculation region was observed, decreasing the swirl separation capability. A further geometry similar to that proposed by Dirkzwager was investigated, where no such problems were observed. Thus, it is clear that the geometry of the cyclone has a decisive influence in the separation performance. The next phase of the research will include simulations with turbulent flow.

Notation

A	cross section area, m^2
A_{in}	annular area, m^2
D	diameter of tubing, m
P	pressure, Pa
P*	dimensionless pressure
P_{rel}	relative pressure, Pa
r	radial coordinate, m
R	radius of the tubing, m
r*	dimensionless radius
r_c	cone radius, m
Re	Reynolds number
r_t	external swirl generator radius, m
S	swirl number
u	tangential velocity, m/s
u*	dimensionless tangential velocity
U_{in}	inlet tangential velocity, m/s
v	radial velocity, m/s
v*	dimensionless radial velocity
w	axial velocity, m/s
w*	dimensionless axial velocity
W_{avg}	average axial velocity, m/s
W_{in}	inlet axial velocity, m/s
z	axial coordinate, m
z*	dimensionless axial coordinate

Greek letters

μ	dynamic viscosity, kg/m/s
ρ	density, kg/m^3
δ*	dimensionless thickness
θ	angular coordinate, rad
α	deflection angle

5. ACKNOWLEDGEMENTS

The authors would like to thank the financial support of CAPES.

6. REFERENCES

Baker,D. W., Sayre Jr., 1971, “Decay of swirling turbulent flow of incompressible fluids in long pipes”, Flow its Measurement and Control in Science and Industry, Proceedings of the ASME Fluids Engineering Conference, v1, pp. 301-312.

Delfos, R., Dirkzwager, M., 1998, “Motion of oil droplets in strongly swirling pipe flow” Proceedings of 3rd International Conference on Multiphase Flow, Lyon, paper 445.

Delfos, R., Murphy, S., Stanbridge, D., Olujic, Z., Jansens, P. J., 2004, “A Design Tool for Optimising Axial Liquid-Liquid Hydrocyclones”, Minerals Engineering, Vol. 17, pp. 721-731. Engineering Science, v62, pp. 1629-1635.

Dirkzwager, M., 1996, “A New axial cyclone design for liquid-liquid separation”, Ph.D. Thesis, Delft University of Technology.

Gupta, A. K., Lilley, D. G., Syred, N., 1984, “Swirl Flows”. Abacus Press, Turnbridge Wells.

Keege, S. J., 2000, “Numerical Simulation of an Axial Hydrocyclone”, M.Sc. Thesis, Delft University of Technology.

Kitoh, O., 1991, “Experimental Study of Turbulent Swirling Flow in a Strainght Pipe”, Jounal of Fluid Mechanics, v225, pp. 445-479.

Murphy, S., Delfos, R., Pourquié, M. J. B. M., Olujic, Z., Jansens, P. J., Nieuwstadt, F. T. M., 2007, “Prediction of Strongly Swirling Flow Within an Axial Hydrocyclones Using Two Commercial CFD Codes”, Chemical Klujszo, L. A. C., Rafaelof, M., Rajamani, R. K., 1999, “Dust Collection Performance of a Swirl Air Cleaner”, Powder Technology, Vol. 103(2), pp. 130-138.

Nieuwstadt, F. T. M, Dirkzwager, M., 1995, “A Fluid Mechanics Model for an Axial Cyclone Separator”, Ind. Engineering Chemical Research, Vol.34, pp.3399-3404.

Patankar, S. V., “Numerical Heat Transfer and Fluid Flow”, Hemisphere, Washington.

Senoo, Y., Nagata, T., 1972, "Swirl Flow in Long Pipes with Different Roughness", Bulletin of the JSME, v15, pp.1514-1521.

Sheen, H. J., Chen, W. J., Jeng, S. Y., Huang, T.L., 1996, "Correlation of swirl number for a radial-type swirl generator". Experimental Thermal and Fluid Science, v12, pp.444-451.

Swanborn, R. A., 1998, "A New Approach to the Design of Gas-Liquid Separators for the Oil Industry", Ph.D. Thesis, Delft University of Technology.

Young, G. A. B., 1994, "Oil-Water Separation Using Hydrocyclone: An Experimental Search for Optimum Dimensions", Journal of Petroleum Science Engineering, Vol 11(1), pp 37-50.

5. RESPONSIBILITY NOTICE

The authors are the only responsible for the printed material included in this paper.